ARMY RESEARCH LABORATORY

Microstructure and Properties of WC Spheres

by Jeffrey J. Swab, Justin Pritchett, Andrew A. Wereszczak, and Osama M. Jadaan

ARL-TR-4634 November 2008

Army Research Laboratory
Aberdeen Proving Ground, MD 21005-5069

ARL-TR-4634 **November 2008**

Microstructure and Properties of WC Spheres

Jeffrey J. Swab
Weapons and Materials Research Directorate, ARL

Justin Pritchett
Oak Ridge Institute for Science and Education

Andrew A. Wereszczak
Oak Ridge National Laboratory

Osama M. Jadaan
University of Wisconsin-Platteville

REPORT DOCUMENTATION PAGE			*Form Approved OMB No. 0704-0188*
Public reporting burden for this collection of information is estimated to average 1 hour per response, including the time for reviewing instructions, searching existing data sources, gathering and maintaining the data needed, and completing and reviewing the collection information. Send comments regarding this burden estimate or any other aspect of this collection of information, including suggestions for reducing the burden, to Department of Defense, Washington Headquarters Services, Directorate for Information Operations and Reports (0704-0188), 1215 Jefferson Davis Highway, Suite 1204, Arlington, VA 22202-4302. Respondents should be aware that notwithstanding any other provision of law, no person shall be subject to any penalty for failing to comply with a collection of information if it does not display a currently valid OMB control number. **PLEASE DO NOT RETURN YOUR FORM TO THE ABOVE ADDRESS.**			
1. REPORT DATE *(DD-MM-YYYY)* November 2008	**2. REPORT TYPE** Final		**3. DATES COVERED (From - To)** January 2006–August 2006
4. TITLE AND SUBTITLE Microstructure and Properties of WC Spheres			**5a. CONTRACT NUMBER** **5b. GRANT NUMBER** **5c. PROGRAM ELEMENT NUMBER**
6. AUTHOR(S) Jeffrey J. Swab, Justin Pritchett,* Andrew A. Wereszczak,† and Osama M. Jadaan‡			**5d. PROJECT NUMBER** 622618H80 **5e. TASK NUMBER** **5f. WORK UNIT NUMBER**
7. PERFORMING ORGANIZATION NAME(S) AND ADDRESS(ES) U.S. Army Research Laboratory ATTN: AMSRD-ARL-WM-MB Aberdeen Proving Ground, MD 21005-5069			**8. PERFORMING ORGANIZATION REPORT NUMBER** ARL-TR-4634
9. SPONSORING/MONITORING AGENCY NAME(S) AND ADDRESS(ES)			**10. SPONSOR/MONITOR'S ACRONYM(S)** **11. SPONSOR/MONITOR'S REPORT NUMBER(S)**
12. DISTRIBUTION/AVAILABILITY STATEMENT Approved for public release; distribution is unlimited.			
13. SUPPLEMENTARY NOTES *Work performed while an undergraduate student at the Harford Community College and with support by an appointment to the Research Participation Program at the U.S. Army Research Laboratory (ARL) administered by the Oak Ridge Institute for Science and Education through an interagency agreement between ARL and the U.S. Department of Energy. †Oak Ridge National Laboratory, Oak Ridge, TN 37831 ‡University of Wisconsin-Plateville, Plateville, WI 53818			
14. ABSTRACT Tungsten carbide (WC) spheres are used as projectiles to study the ballistic performance of armor materials and systems. In order to properly understand and model the interaction between the projectile and the armor, it is necessary to have properties of both. In this study, the physical and mechanical properties of two commercially available WC spheres (nominally 0.25 inch in diameter) used in some ballistic impact studies were determined. One WC sphere had higher density, elastic properties, and hardness but lower strength and fracture toughness compared to the other sphere, indicating a significant difference in the binder content between the two materials.			
15. SUBJECT TERMS tungsten carbide, strength, elastic modulus, spheres, microstructure			

16. SECURITY CLASSIFICATION OF:			**17. LIMITATION OF ABSTRACT**	**18. NUMBER OF PAGES**	**19a. NAME OF RESPONSIBLE PERSON** Jeffrey J. Swab
a. REPORT UNCLASSIFIED	**b. ABSTRACT** UNCLASSIFIED	**c. THIS PAGE** UNCLASSIFIED	SAR	32	**19b. TELEPHONE NUMBER** (*Include area code*) 410-306-0753

Standard Form 298 (Rev. 8/98)
Prescribed by ANSI Std. Z39.18

Contents

List of Figures

List of Tables

INTENTIONALLY LEFT BLANK.

1. Introduction

Tungsten carbide (WC)-based materials are probably best known as "cutting tools" since these materials have been commercially available for a variety of metal cutting and rock drilling operations since the early part of the 20th century. These materials are also used extensively as abrasive grits and in wear resistant components. WC has been considered as a potential vehicle armor because it possesses a number of characteristics (high hardness, stiffness, strength, and toughness) desired of an armor ceramic while possibly offering the required ballistic performance in a thinner armor package (*1–3*). Conversely, it is also a preferred material for the core component of several armor piercing projectiles because of several of these same characteristics (*4*).

Most WC products are fabricated by liquid phase sintering of a powder mixture containing WC particles and a metallic binder. Products produced in this manner are typically classified as "cermets" or "cemented carbides" due to the fact that the binder is located at WC grain boundaries and multigrain junctions effectively "cementing" the WC particles together. Cobalt (Co) and Co-based alloys are the most widely used binders, with WC-based products containing up to 30 weight-percent Co readily available as a commercial product (*5*).

In order to better understand the impact resistance of advanced ceramics many research efforts have used WC spheres (*6, 7*) and rods (*8*) as the impacting projectile. The ability to properly model a ballistic impact event requires knowledge of the properties of both the target and the projectile material. This report summarizes the characterization of two WC spheres that have been used as projectiles in some impact studies.

2. Experimental Procedure

Commercially available, 0.25-in- (6.35-mm)-diameter WC spheres were obtained from New Lenox Machine, Co., Inc.[*] (NL) and Machining Technologies Inc.[†] (MT). The NL supplied spheres are machined from WC blanks supplied by an outside manufacturer while MT spheres are pressed, sintered, and machined entirely at their facility.

A sphere from each vendor was cut in half then mounted and polished to a 0.05-µm finish, using a colloidal silica solution. These specimens were used for hardness testing and examination of the microstructure. Microstructural images were obtained from a scanning electron microscope (SEM) to determine the grain size following the procedure outlined in ASTM E 112 (*9*). Knoop

* New Lennox Machine Co., Inc., 1200 E. Mazon Ave., Dwight, IL 60420
† Machining Technologies, Inc., 468 Maple St., Elmore, OH 43416-0287

and Vickers hardness values both were determined using a Wilson Instruments Tukon* 300 microhardness tester according to the procedures in ASTM C 1326-96a (*10*) and ASTM C 1327-96 (*11*), respectively. Knoop hardness testing was conducted across a range of loads between 0.49 and 98.1 N to determine if the indentation size effect was present in either WC. Vickers testing was done solely at 9.8 N at the edge and centers of the cross-sectioned sphere to determine if the hardness was consistent throughout the sphere.

The elastic and shear modulus as well as the Poisson's ratio were determined using resonance ultrasound spectroscopy (RUS) using a method described elsewhere (*12*). Briefly, their measurement is a consequence of the combination of the identification of resonant frequencies, sphere diameter, material density, and modal analysis via finite element modeling. The resonant frequencies were measured with a commercial resonant ultrasound spectroscope (Quasar International, Inc.)† and the modal analysis performed using ANSYS.‡ This method can produce an accurate estimate of elastic modulus and Poisson's ratio that are independently determined (i.e., an assumption of one is not needed to estimate the other).

Twenty-five spheres of each material were machined to C-shaped specimens by Bomas Machine Specialties Co.§ for strength testing. The dimensions of the C-sphere specimens are shown in figure 1. Strength testing was performed on an Instron** model 5500 universal test frame following the procedures outlined by Wereszczak et al. (*13*). Fractography was performed on the fracture surfaces of these specimens using an optical microscope following the details discussed in ASTM C 1322 (*14*). High resolution/high magnification imaging of the fracture origin and surrounding area was also performed on select specimens using a SEM to identify fracture origins and fracture mechanisms.

3. Results and Discussion

3.1 Microstructure

The microstructure of each material is shown in figure 2 (NL) and figure 3 (MT). The microstructure of the NL material is consistent across the diameter of the sphere. There is evidence of some variability in the grain size as the microstructure consists primarily of grains in the 2–3-µm size range with large grains (up to 10 µm) distributed throughout.

* Tukon is a registered trademark of Wilson Instruments, a division of Instron Corporation, 825 University Ave., Norwood, MA 02062-2643.

† Quasar International, Inc., Albuquerque, NM

‡ ANSYS, Canonsburg, PA

§ Bomas Machine Specialties Co., 334 Washington St., Somerville, MA 02134

** Instron Corporation, 825 University Ave., Norwood, MA 02602-2643

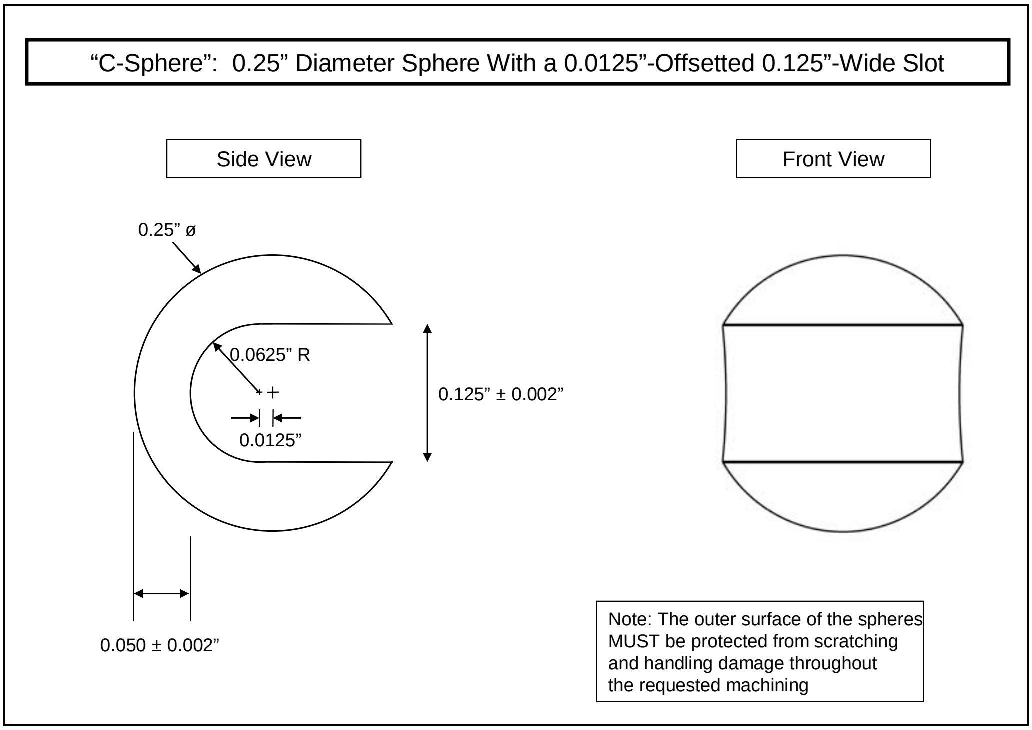

Figure 1. Schematic of the C-sphere specimen.

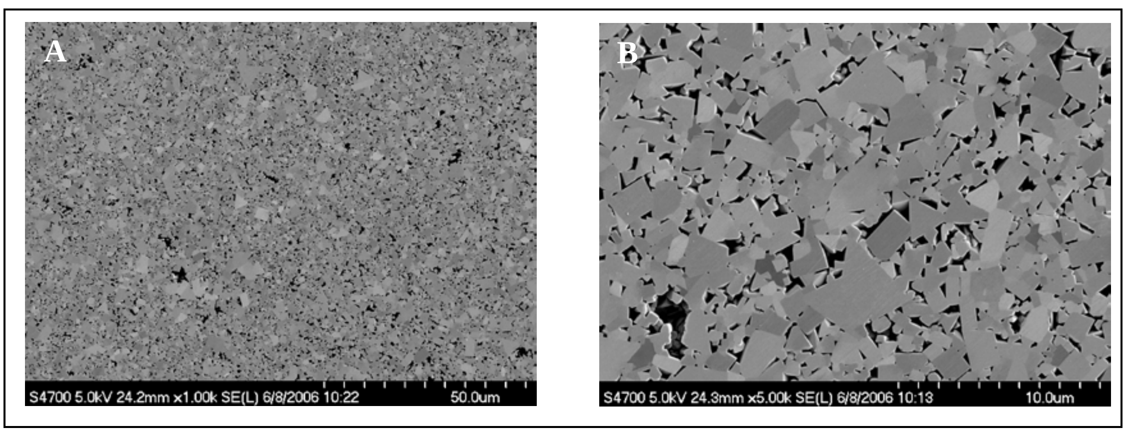

Figure 2. Microstructure of NL WC. The bimodal grain size can be see in (a) while (b) clearly shows the void space (porosity) between the WC grains.

The MT material, on the other hand, has a much finer overall grain size but there is a change in the microstructure, about 125 μm below the sphere surface. The depth below the surface where this change occurs is uniform around the sphere perimeter. The change is a noticeable increase in the amount and size of the porosity as well as a possible, albeit slight, increase in grain size (≈0.3 μm to ≈0.35 μm). An energy dispersive spectra (EDS) analysis of each area showed no change in the W and C content on either side of this boundary nor were there any differences in the elemental content.

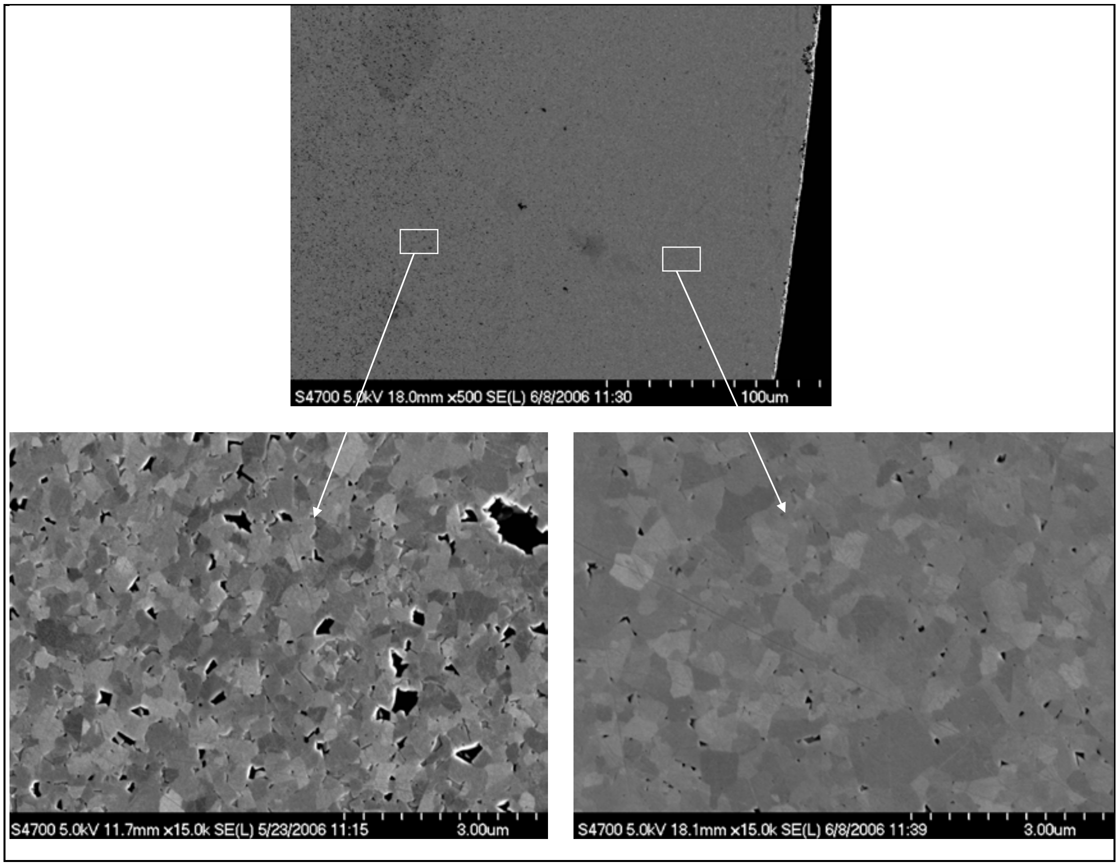

Figure 3. Microstructure of MT WC. The top image shows the change in microstructure from the surface in to the middle of the sphere. The bottom pair of images clearly shows the difference in the size and amount of porosity in the two areas.

3.2 Physical and Mechanical Properties

The physical and mechanical properties of these WC spheres are summarized in table 1 while raw data can be found in the appendix.

3.2.1 Physical Properties

The density and elastic properties indicate a difference in the binder content of these two WC materials. The density and moduli of the MT WC are all appreciably higher than the NL WC. The values for the MT WC are in excellent agreement with a material that is essentially a "pure" or "binderless" WC. Conversely the property values for the NL WC show that a binder, probably around 6%, was added to this material. The addition of a binder, such as Co, typically results in lowering the density, elastic properties and hardness while increasing strength and toughness.

Table 1. Physical and mechanical property summary.

	New Lenox	Machining Technologies
Density (g/cm^3)	14.80 ± 0.01	15.61 ± 0.02
Elastic properties		
▪ Youngs modulus (GPa)	613.5 ± 1.0	679.4 ± 2.1
▪ Shear modulus (GPa)	252.7 ± 0.4	282.4 ± 1.1
▪ Bulk modulus (GPa)	357.2 ± 0.7	380.9 ± 0.3
▪ υ	0.2138 ± 0.0	0.2027 ± 0.0
Strength (MPa)		
▪ Average	3581 ± 162 (24)[a]	3152 ± 241 (25)
▪ Characteristic	3652[b]	3262
Unbiased Weibull modulus[c]	28.6	14.8
Vickers hardness (1 kg) (GPa)		
▪ Sphere center	14.4 ± 0.2	24.5 ± 0.4
▪ Sphere edge	14.2 ± 0.5	22.9 ± 0.9

[a]Number in parenthesis indicates the number of specimens tested.
[b]Weibull characteristic strength associated with the test specimen.
[c]Determined using a 2-parameter maximum likelihood estimation and 95% confidence bounds.

3.2.2 Hardness

The Vickers hardness at a 1000 g (9.81 N) load was appreciably different for these two materials. The hardness of the MT material was determined near the edge and in the middle of the sphere due to the microstructural change that was observed. The hardness in the middle of the sphere was 24.5 ± 0.4 GPa, while at the edge it was slightly lower at 22.9 ± 0.9 GPa. The NL WC was softer but had a consistent hardness across the sphere diameter. At the edge, the Vickers hardness was 14.2 ± 0.5 GPa and in the middle it was 14.4 ± 0.2 GPa.

Since the NL WC exhibited a consistent microstructure across the sphere diameter additional hardness testing was done to develop a hardness/load curve to determine if the indentation size effect (ISE) was present. This phenomenon is exhibited by a material when at very low indentation loads the hardness is usually quite high but as the load decreases the hardness also decreases until a load is reached where the hardness becomes essentially load-independent (*15–18*). Both Vickers and Knoop hardness values were determined between 50 g (0.49 N) and 10 kg (98.1 N). The Vickers indentations at 0.49 N were slightly larger than 8 µm in size and difficult to measure accurately. The average hardness was only 13.3 GPa, but with a very high standard deviation of 1.4 due to the small size of the indents and the resolution of the objective lenses. At 0.98 N, the hardness jumped to 14.7 GPa and remained essentially at this value as the indentation load was increased to 98.1 N indicating that the ISE was not present. However, the Knoop hardness/load profile showed the exact opposite behavior—that the ISE was quite evident. The hardness was 17.0 ± 0.6 GPa at 0.49 N but gradually dropped to ~13.5 GPa at 9.8 N and remained at this value up to the maximum load of 98.0 N. Earlier work (*18*) showed the same behavior in two other WC materials, but there is no clear explanation for this difference in hardness/load behavior based on indenter geometry.

3.2.3 Strength

The characteristic strength and unbiased Weibull modulus of each WC material was determined using a 2-paramenter Weibull analysis with 95% confidence bounds. The effective area and effective volume as a function of Weibull modulus were computed and are shown in figures 4 and 5. The effect of the ligament thickness (between 1.15 and 1.30 mm) on the maximum tensile stress was also examined, figures 6 and 7. There was a strong correlation between the finite element and linear regression analysis (correlation coefficient of 0.998 in both cases). This coupled with the fact that the average ligament thickness for both materials was well within the analyzed range (NL: 1.223 ± 0.032 mm; MT: 1.265 ± 0.115 mm) indicated that there was no need to correct the measured strength values.

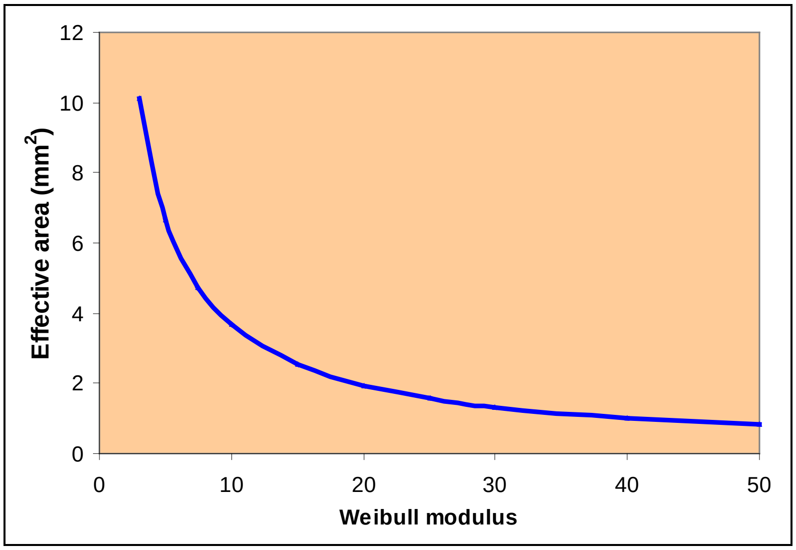

Figure 4. Effective area vs. Weibull modulus for the 6.35-mm-diameter C-sphere specimen with 1.27-mm ligament thickness.

The characteristic strength of the NL WC was ~12% higher than the MT WC. The presence of a binder in the NL will account for this difference. However, the significantly higher Weibull modulus (28.6 for NL compared to 14.9 for MT) cannot be attributed to a difference in binder content.

3.2.4 Fractography

An analysis of the fractured specimens revealed that fracture initiated in all of the c-sphere specimens within the general vicinity of the most highly stressed area on the sphere, based on the previous analysis conducted (*13*). Detailed fractography of the fracture surfaces showed a significant difference in flaw types present in each WC. The strength of the NL WC was limited primarily by machining damage that was probably introduced during the sphere fabrication process. This flaw was present at the surface and typically had a semi-elliptical shape. An example can be seen in figure 8. While machining damage was the primary origin, occasionally clusters of large WC grains limited the strength of some spheres, figure 9.

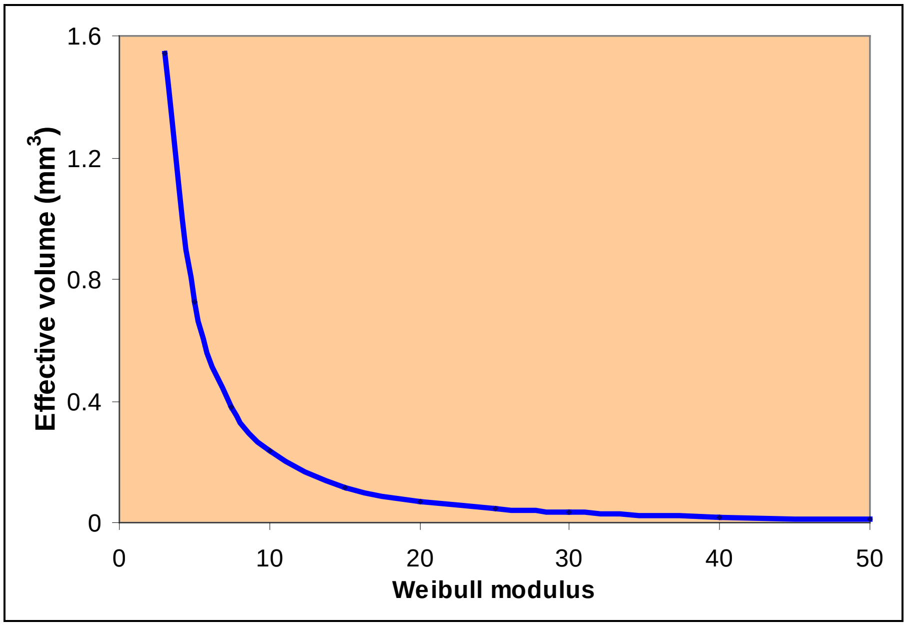

Figure 5. Effective volume vs. Weibull modulus for the 6.35-mm-diameter C-sphere specimen with 1.27-mm ligament thickness.

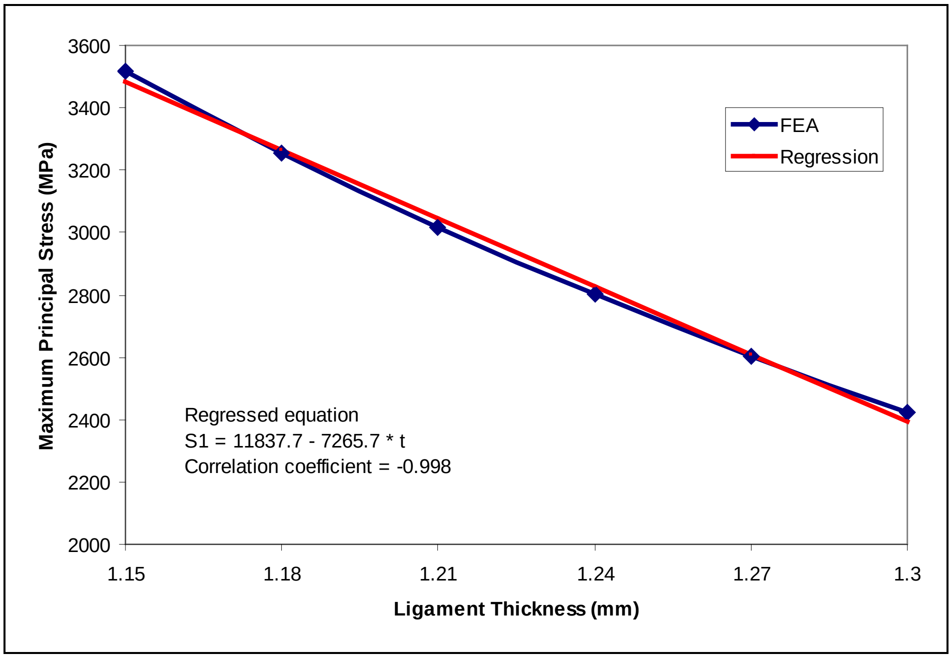

Figure 6. Maximum tensile stress vs. ligament thickness for the 6.35-mm-diameter MT WC C-sphere specimen configuration due to an applied load of 1000 N.

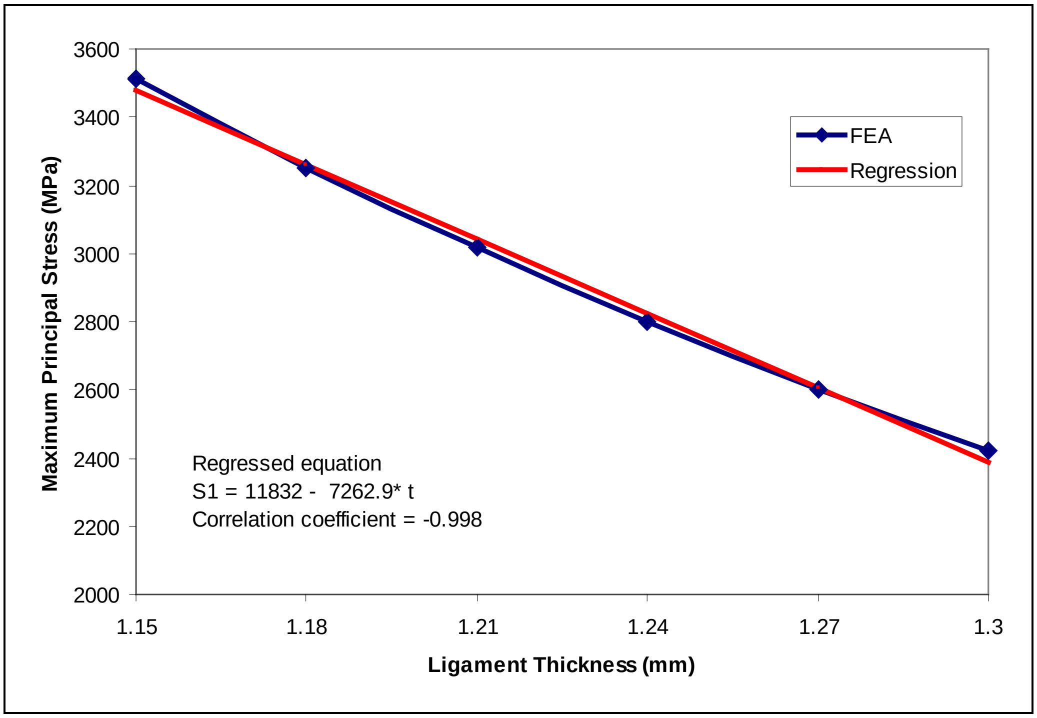

Figure 7. Maximum tensile stress vs. ligament thickness for the 6.35-mm-diameter NL WC C-sphere specimen configuration due to an applied load of 1000 N.

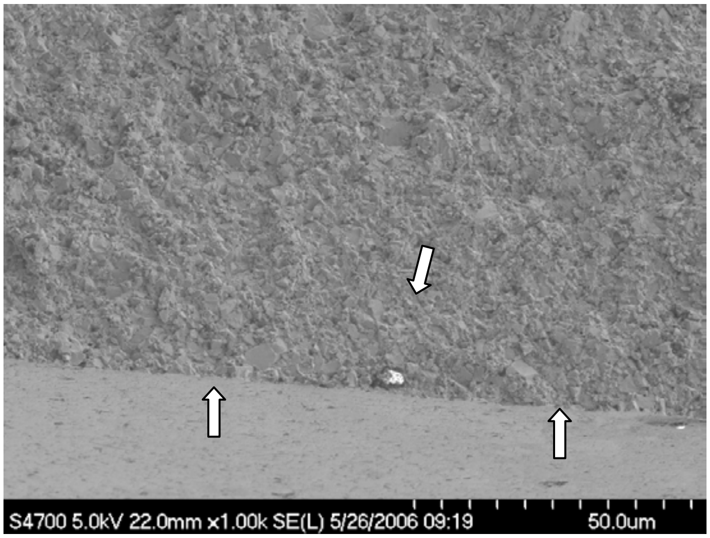

Figure 8. Example of the primary strength-limiting flaw in the NL WC sphere. The white arrows highlight length and depth of the machining crack that was probably introduced during the sphere fabrication process. C-sphere no. 7; σ = 3543 MPa; origin characterization (MD, S, 30 × 110 μm).

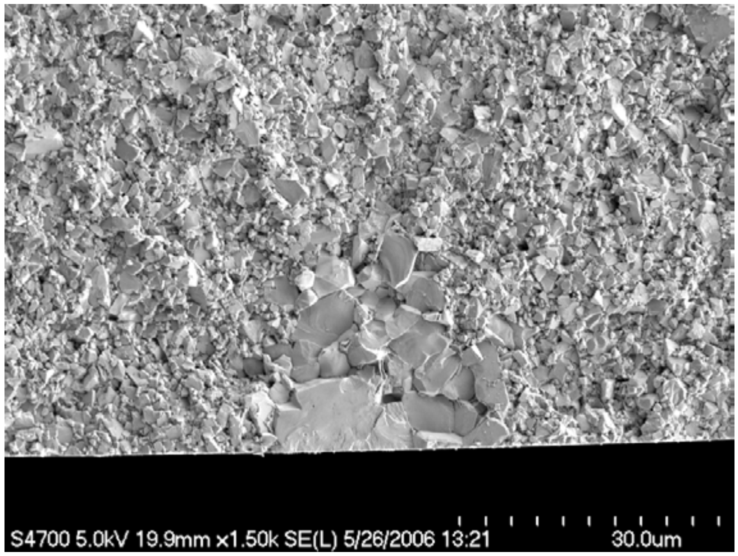

Figure 9. Cluster of large WC grains limited the strength of NL c-sphere no. 18. σ = 3429 MPa; origin characterization (LG, S, 30 μm).

The fracture of the MT WC spheres was due exclusively to volume-distributed pores located well beneath the C-sphere surface, as shown in figures 10 and 11. Some of these pores were quite obvious and could easily be measured at low magnifications (figure 10), while a higher power magnification was needed in some instances to confirm the presence of the pore (figure 11). In the later instance, the appearance of large grains in the area confirm that this must have been a pore. The open space from the pore provided an unconstrained area for grain growth to occur during sintering. The location of these strength-limiting pores is in excellent agreement with the previously described analysis of the microstructure which showed that there was an increase in the amount and size of the porosity ~125 μm beneath the sphere surface.

3.2.5 Fracture Toughness

The small diameter of the WC sphere precluded the direct determination of a K_{Ic} value but a fracture toughness estimate was determined fractographically. Six of the fracture MT C-sphere specimens had origins that could easily and accurately be measured. The toughness range for this WC was 6.7–11.2 MPa√m, which is in good agreement with the toughness reported for other "binderless" WC materials (*3*). The toughness range for the NL material was 21.6–29.8 MPa√m. This difference is not surprising since the addition of a binder yields a WC material with a significantly higher fracture toughness.

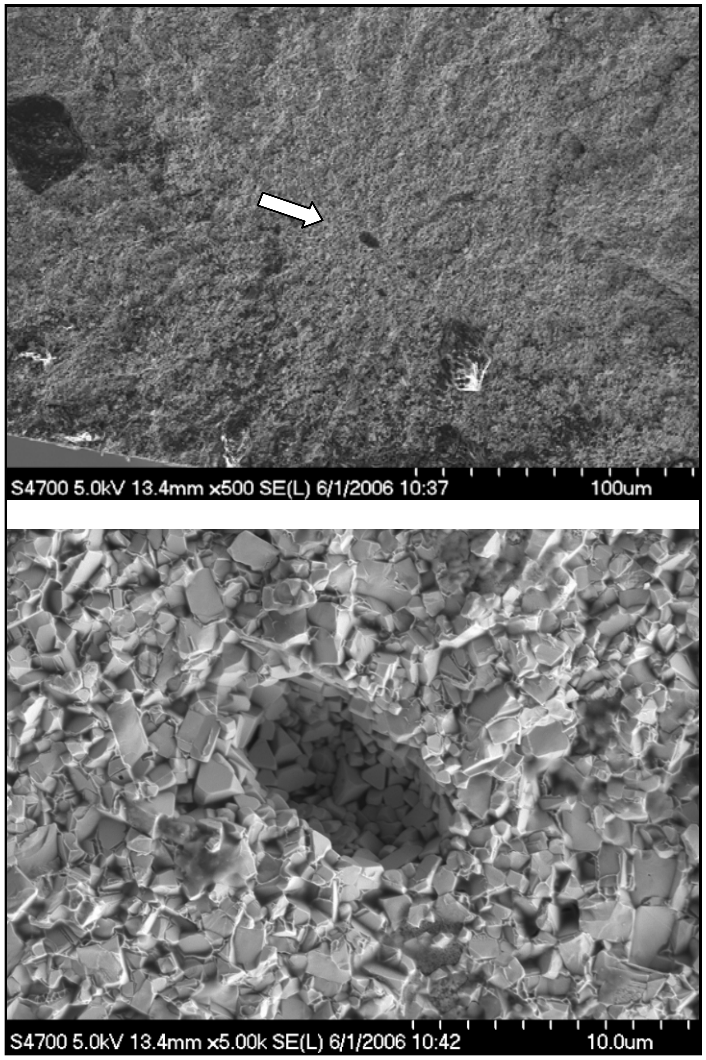

Figure 10. SEM images of the fracture origin in MT C-sphere no. 8. Top: low-magnification image of an elliptical pore located ~100 µm below the surface. Bottom: high-magnification image of the pore. σ = 3521 MPa; origin characterization (P, V, 5 × 10 µm).

4. Summary

The physical and mechanical properties of two commercially-available WC spheres (NL and MT) used in some ballistic impact studies (*6, 7*) were determined. The NL WC had a significantly higher strength and toughness than the MT WC due to the presence of a binder while the MT WC was denser and harder while having higher elastic property values indicating a significant difference the amount of binder phase present. The microstructure of the MT WC revealed that there was an increase in the size and amount of porosity ~125 µm beneath the

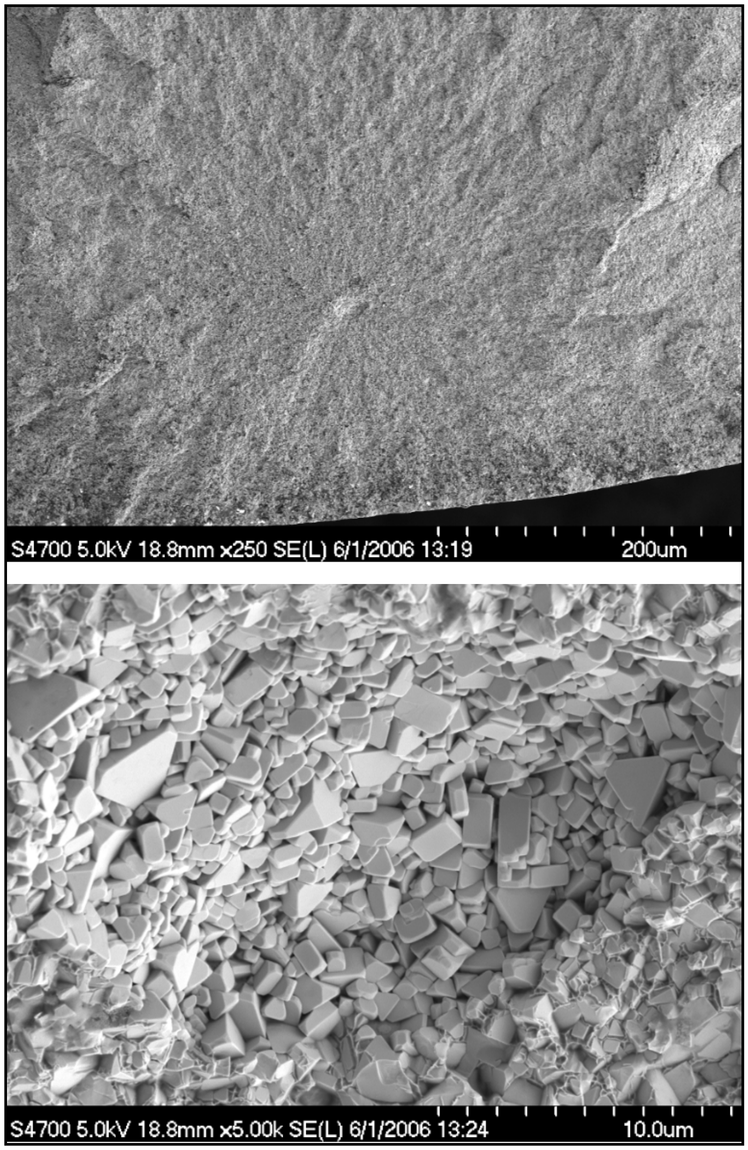

Figure 11. SEM images of the fracture origin in MT C-sphere no. 19. Top: low-magnification image of a pore located ~200 μm below the surface. Bottom: high-magnification image of the pore. σ = 2828 MPa; origin characterization (P, V, 25 μm).

sphere surface. This change in microstructure limited the strength of the spheres as subsurface pores were the primary fracture origin in this material. It is important to know the differences between these spheres as some of this WC property data may be incorporated into ballistic codes that analyze and predict the performance of armor systems.

5. References

1. Rupert, N. L.; Schoon, R. J. Evaluation of High-Density Ceramics for Ballistic Applications. *Proceedings on Dynamic Loading in Manufacturing and Service,* Melbourne, Victoria, Australia, 199–205, February 1993.

2. Gooch, W. A.; Burkins, M. S.; Palicka, R. Ceramic Armor Materials by Design. Ballistic Development of High Density Tungsten Carbide Ceramics; In *Ceramic Transactions,* Vol. 134, McCauley, J. W., Crowson, A., Gooch, W. A., Jr., Rajendran, A. M., Bless, S. J., Logan, K.V., Normandia, M., Wax, S., Eds.; American Ceramic Society: Westerville, OH, 2002; pp 53–61.

3. Swab, J. J.; Tice, J. *Evaluation of Tungsten Carbide (WC) for Armor Applications;* ARL-TR-3523; U.S. Army Research Laboratory: Aberdeen Proving Ground, MD, June 2005.

4. Armor Piercing Projectiles. U.S. Patent 4108073.

5. Stevenson, R. W. Cemented Carbides. *Metals Handbook – Ninth Edition;* Vol. 7; *Powder Metallurgy* **1984**, 774–783.

6. Normandia, M.; Leavy, B. Ballistic Impact of Silicon Carbide with Tungsten Carbide Spheres. *Ceram. Eng. Sci. Proc.* 2004, *25* (3), 573–578.

7. Normandia, M. R.; Martin, S. R.; MacKenzie, D. E.; Rickter, B. A Comparison of Ceramic Materials 8 Dynamically Impacted by Tungsten Carbide Spheres. *Ceram. Eng. Sci. Proc.* **2005**, *26* (7), 203–214.

8. Orphal, D. L.; Franzen, R. R.; Charters, A. C.; Menna, T. L., Piekutowski, A. J. Penetration of Confined Boron Carbide Targets by Tungsten Long Rods at Impact Velocities from 1.5 to 5.0 km/s. *Int. J. Impact Eng*. **1997**, *19* (1), 15–29.

9. ASTM E 112. Standard Test Method for Determining Average Grain Size. *Annu. Book ASTM Stand*. **2004**, Vol. 03.01.

10. ASTM C 1326-96a. Standard Test Method for Knoop Indentation Hardness of Advanced Ceramics. *Annu. Book ASTM Stand*. **2005**, Vol. 15.01.

11. ASTM C 1327-96a. Standard Test Method for Vickers Indentation Hardness of Advanced Ceramics. *Annu. Book ASTM Stand*. **2005**, Vol. 15.01.

12. Wereszczak, A. A. Elastic Property Determination of WC Spheres and Estimation of Compressive Loads and Impact Velocities That Initiate Their Yielding and Cracking. *Ceram. Eng. Sci. Proc.* **2006**, *27* (7), 211–223.

13. Wereszczak, A. A.; Kirkland, T. P.; Jadaan, O. M. Strength Measurement of Ceramic Spheres Using a Diametrally Compressed C-Sphere Specimen. *J. Am. Ceram. Soc.* **2007**, *90* (6), 1843–1849.

14. ASTM C 1322. Standard Practice for Fractography and Characterization of Fracture Origins in Advanced Ceramics. *Annu. Book ASTM Stand*. **2005**, Vol. 15.01.

15. Li, H.; Bradt, R. C. The Indentation Load/Size Effect and the Measurement of the Hardness of Vitreous Silica. *J. Non-Cryst. Sol*. **1992**, *146*, 197–212.

16. Li, H.; Bradt, R. C. The Microhardness Indentation Size-Load Effect (ISE) in Hard Ceramic Materials. *J. Hard Mat.* **1992**, *23* (3–4), 403–419.

17. Quinn, J. B.; Quinn, G. D. Indentation Brittleness of Ceramics: A Fresh Approach. *J. Mat. Sci.* **1997**, *32*, 4331–4336.

18. Swab, J. J. Recommendations for Determining the Hardness of Armor Ceramics. *Int. J. Appl. Ceram. Technol.* **2004**, *1* (3), 219–225.

INTENTIONALLY LEFT BLANK.

Appendix. Raw Data – Physical and Mechanical Properties

Table A-1. Density and elastic properties.

No.	Mass (g)	Diameter (mm)	Density (g/cm^3)	Young's Modulus (GPa)	Poisson's Ratio	Shear Modulus (GPa)	Bulk Modulus (GPa)
New Lenox							
1	1.9820	6.349	14.79	613.1	0.2137	252.6	356.9
2	1.9829	6.349	14.80	614.6	0.2134	253.3	357.4
3	1.9825	6.349	14.79	612.9	0.2138	252.5	356.9
4	1.9820	6.349	14.79	612.9	0.2138	252.5	356.9
5	1.9818	6.348	14.80	612.9	0.2140	252.4	357.2
6	1.9823	6.348	14.80	613.0	0.2138	252.5	357.0
7	1.9827	6.349	14.80	614.3	0.2138	253.0	357.7
8	1.9822	6.349	14.79	613.1	0.2138	252.6	357.0
9	1.9825	6.349	14.79	613.3	0.2140	252.6	357.4
10	1.9825	6.348	14.80	614.5	0.2138	253.1	357.8
	AVG	6.349	14.80	613.5	0.2138	252.7	357.2
	STD	0.001	0.008	0.990	0.000	0.393	0.665
Machining Technologies							
1	2.0959	6.355	15.60	678.8	0.2022	282.3	379.9
2	2.0959	6.356	15.59	679.8	0.2022	282.7	380.5
3	2.0984	6.356	15.61	680.0	0.2035	282.5	382.2
4	2.0997	6.355	15.62	679.5	0.2035	282.3	382.0
5	2.0982	6.355	15.61	683.2	0.2017	284.3	381.7
6	2.0996	6.356	15.62	680.0	0.2025	282.7	381.0
7	2.1008	6.356	15.63	677.6	0.2046	281.3	382.3
8	2.1006	6.355	15.63	676.6	0.2028	281.3	379.4
9	2.0977	6.356	15.60	676.7	0.2035	281.1	380.4
10	2.0988	6.355	15.62	681.7	0.2006	283.9	379.5
	AVG	6.356	15.61	679.4	0.2027	282.4	380.9
	STD	0.000	0.015	2.051	0.001	1.120	0.294

Table A-2. Strength of new Lenox.

New Lenox				
Sample No.	**Lig. Thick (mm)**	**OD (mm)**	**Max. Load (N)**	**σ_{max} (MPa)**
20	1.232	6.351	1053	3159
5	1.211	6.347	1098	3294
19	1.217	6.350	1110	3330
18	1.246	6.350	1143	3429
1	1.279	6.349	1144	3432
21	1.209	6.351	1160	3480
3	1.204	6.336	1179	3537
7	1.235	6.347	1181	3543
25	1.234	6.349	1186	3558
9	1.229	6.347	1190	3570
13	1.229	6.348	1205	3615
14	1.259	6.349	1205	3615
2	1.797	6.348	1207	3621
16	1.271	6.350	1211	3633
23	1.212	6.350	1216	3648
6	1.297	6.347	1221	3663
4	1.276	6.340	1223	3669
22	1.284	6.350	1224	3672
10	1.228	6.348	1231	3693
17	1.263	6.350	1234	3702
12	1.190	6.348	1250	3750
15	1.284	6.347	1250	3750
8	1.225	6.347	1253	3759
24	1.295	6.350	1273	3819
11	1.212	6.348	Broke during preload	
AVG	1.265	6.348	1193.6	3580.9
STD	0.115	0.003	53.4	160.1

Table A-3. Strength of machining technologies.

Machining Technologies				
Sample No.	**Lig. Thick (mm)**	**OD (mm)**	**Max. Load (N)**	**σ_{max} (MPa)**
18	1.184	6.348	892.4	2679
1	1.191	Not measured	931.9	2798
11	1.182	6.345	933.5	2802
19	1.219	6.347	941.9	2828
12	1.234	6.346	956.5	2871
22	1.268	6.348	965.8	2899
20	1.189	6.349	997.3	2994
13	1.201	6.348	1001.0	3005
10	1.241	6.345	1017.0	3053
14	1.227	6.347	1042.0	3128
4	1.247	6.345	1050.0	3152
2	1.272	6.346	1053.0	3161
5	1.250	6.346	1062.0	3188
25	1.231	6.348	1064.0	3194
17	1.206	6.348	1068.0	3206
21	1.247	6.348	1095.0	3287
23	1.197	6.348	1101.0	3305
7	1.241	6.346	1104.0	3314
6	1.196	6.345	1109.0	3329
9	1.223	6.346	1110.0	3332
24	1.161	6.348	1126.0	3380
15	1.243	6.346	1136.0	3410
16	1.216	6.348	1141.0	3425
8	1.217	6.346	1173.0	3521
3	1.292	6.345	1177.0	3533
AVG	1.223	6.347	1049.9	3151.9
STD	0.032	0.001	80.2	240.6

Table A-4. Vickers hardness of new Lenox and machining technologies (middle).

New Lenox				
	gf	N		
Load =	1000	9.81		
Indent No.	Ave d (µm)	Ave d (mm)	HV	HV (GPa)
1	35.6	0.0356	1463.2	14.3
2	35.7	0.0357	1455.0	14.3
3	35.6	0.0356	1463.2	14.3
4	35.1	0.0351	1505.2	14.8
5	35.8	0.0358	1446.9	14.2
AVG	35.6	0.0356	1466.7	14.4
STD	0.3	0.0003	22.6	0.2
Machining Technologies				
	gf	N		
Load =	1000	9.81		
Indent No.	Ave d (µm)	Ave d (mm)	HV	HV (GPa)
1	27.4	0.0274	2470.0	24.2
2	26.8	0.0268	2581.9	25.3
3	27.3	0.0273	2488.2	24.4
4	27.2	0.0272	2506.5	24.6
5	27.7	0.0277	2416.8	23.7
6	27.3	0.0273	2488.2	24.4
7	27.0	0.0270	2543.8	24.9
8	27.3	0.0273	2488.2	24.4
9	27.5	0.0275	2452.1	24.0
10	27.2	0.0272	2506.5	24.6
AVG	27.3	0.0273	2494.2	24.5
STD	0.2	0.0002	45.8	0.4

Table A-5. Vickers hardness of new Lenox and machining technologies (edge).

New Lenox				
	gf	N		
Load =	1000	9.81		
Indent No.	Ave d (μm)	Ave d (mm)	HV	HV (GPa)
1	35.7	0.0357	1455.0	14.3
2	36.9	0.0369	1361.9	13.4
3	35.6	0.0356	1463.2	14.3
4	35.5	0.0355	1471.5	14.4
5	35.4	0.0354	1479.8	14.5
AVG	35.8	0.0358	1446.3	14.2
STD	0.6	0.0006	48.1	0.5
Machining Technologies				
	gf	N		
Load =	1000	9.81		
Indent No.	Ave d (μm)	Ave d (mm)	HV	HV (GPa)
1	28.0	0.0280	2365.3	23.2
2	27.7	0.0277	2416.8	23.7
3	29.0	0.0290	2205.0	21.6
4	29.1	0.0291	2189.9	21.5
5	28.1	0.0281	2348.5	23.0
6	27.4	0.0274	2470.0	24.2
7	28.2	0.0282	2331.9	22.9
8	28.1	0.0281	2348.5	23.0
9	28.7	0.0287	2251.3	22.1
10	27.6	0.0276	2434.4	23.9
AVG	28.2	0.0282	2336.2	22.9
STD	0.6	0.0006	94.9	0.9

NO. OF COPIES	ORGANIZATION
1 (PDF only)	DEFENSE TECHNICAL INFORMATION CTR DTIC OCA 8725 JOHN J KINGMAN RD STE 0944 FORT BELVOIR VA 22060-6218
1	DIRECTOR US ARMY RESEARCH LAB IMNE ALC IMS 2800 POWDER MILL RD ADELPHI MD 20783-1197
1	DIRECTOR US ARMY RESEARCH LAB AMSRD ARL CI OK TL 2800 POWDER MILL RD ADELPHI MD 20783-1197
1	DIRECTOR US ARMY RESEARCH LAB AMSRD ARL CI OK PE 2800 POWDER MILL RD ADELPHI MD 20783-1197
	ABERDEEN PROVING GROUND
1	DIR USARL AMSRD ARL CI OK TP (BLDG 4600)

NO. OF COPIES	ORGANIZATION
1	DIRECTOR US ARMY RSRCH LAB AMSRD ARL SE DE R ATKINSON 2800 POWDER MILL RD ADELPHI MD 20783-1197
9	DIRECTOR US ARMY RSRCH LAB AMSRD ARL WM MB A ABRAHAMIAN M BERMAN M CHOWDHURY A FRYDMAN R KARGUS T LI J PRITCHETT (3 CPS) 2800 POWDER MILL RD ADELPHI MD 20783-1197
1	COMMANDER US ARMY MATRL CMND AMXMI INT 9301 CHAPEK RD FORT BELVOIR VA 22060-5527
1	US ARMY TARDEC AMSRD TAR R D TEMPLETON 6501 E 11 MILE RD MS 263 WARREN MI 48397-5000
4	US ARMY RSRCH OFC J PRATER D STEPP D KISEROW W MULLINS PO BOX 12211 RESEARCH TRIANGLE PARK NC 27709-2211
1	OFC OF NAVAL RSRCH J CHRISTODOULOU ONR CODE 332 800 N QUINCY ST ARLINGTON VA 22217-5600
2	DARPA S WAX L CHRISTODOULOU 3701 N FAIRFAX DR ARLINGTON VA 22203-1714

NO. OF COPIES	ORGANIZATION
1	DIRECTOR NGIC IANG TMT 2055 BOULDERS RD CHARLOTTESVILLE VA 22091-5391
1	ALLIANT TECHSYSTEMS INC R DOHRN MN07 LW54 5050 LINCOLN DR EDINA MN 55436
2	ALLIANT TECHSYSTEMS INC C AAKHUS D KAMDAR MN07 LW54 5050 LINCOLN DR EDINA MN 55436
1	ALLIANT TECHSYSTEMS INC M JANTSCHER MN07 LW54 5050 LINCOLN DR EDINA MN 55436
1	ALLIANT TECHSYSTEMS INC R BECKER MN11 2626 5050 LINCOLN DR EDINA MN 55340-1097
2	DIRECTOR LLNL S DETERESA F MAGNESS PO BOX 808 LIVERMORE CA 94550
2	GENERAL DYNAMICS OTS FLINCHBAUGH DIV K LINDE G KURZIK PO BOX 127 RED LION PA 17356
3	OAK RIDGE NATIONAL LAB A WERESZCZAK PO BOX 2008 BLDG 4515 MS 6068 OAK RIDGE TN 37831-6068

NO. OF COPIES	ORGANIZATION
1	NATIONAL INSTITUTE OF STANDARDS AND TECHLGY CERAMICS DIV G D QUINN GAITHERSBURG MD 20899
1	THE PENNSYLVANIA STATE UNIV DEPT OF ENGR SCI & MECH 212 EARTH & ENGR SCI BLDG A SEGALL UNIVERSITY PARK PA 16802-6812
1	NASA-GLENN RSRCH CTR LIFE PREDICTION BR MS 49-7 J SALEM CLEVELAND OH 44135
1	KENNAMETAL INC R YECKLEY 1600 TECHLGY WAY LATROBE PA 15650
1	THE PENNSYLVANIA STATE UNIV COLLEGE OF EARTH MINERAL SCI J HELLMANN 14 DIEKE BLDG UNIVERSITY PARK PA 16802
3	UNIV OF WISCONSIN-PLATTEVILLE COLLEGE OF ENGR MATH & SCIENCE O JADAAN PLATTEVILLE WI 53818
1	DIRECTOR US ARMY RESEARCH LABORATORY AMSRD ARL CI J GOWENS 2800 POWDER MILL RD ADELPHI MD 20783-1197

ABERDEEN PROVING GROUND

NO. OF COPIES	ORGANIZATION
1	US ARMY ATC CSTE DTC AT AD I W FRAZER 400 COLLERAN RD APG MD 21005-5059
67	DIR USARL AMSRD ARL O AP EG FI M ADAMSON AMSRD ARL WM J SMITH S KARNA J MCCAULEY P PLOSTINS T WRIGHT AMSRD ARL WM B M ZOLTOSKI J NEWILL AMSRD ARL WM M S MCKNIGHT J BEATTY R DOWDING H MAUPIN AMSRD ARL WM MA M VANLANDINGHAM AMSRD ARL WM MB J BENDER T BOGETTI L BURTON R CARTER W DE ROSSET W DRYSDALE R EMERSON D HOPKINS R KASTE L KECSKES E KLIER M MINNICINO B POWERS D SNOHA J SOUTH J SWAB (20 CPS) J TZENG AMSRD ARL WM MC M MAHER AMSRD ARL WM MD E CHIN J ADAMS J CAMPBELL B CHEESEMAN J LASALVIA J MONTGOMERY AMSRD ARL WM T P BAKER AMSRD ARL WM TA B LEAVY C HOPPEL

NO. OF
COPIES ORGANIZATION

AMSRD ARL WM TC
G BOYCE
L MAGNESS
B SCHUSTER
AMSRD ARL WM TD
T BJERKE
D CASEM
T WEERASOORIYA
AMSRD ARL WM TE
B RINGERS